



Article

# NPA-Cu<sup>2+</sup> Complex as a Fluorescent Sensing Platform for the Selective and Sensitive Detection of Glyphosate

Fang Sun <sup>1,†</sup>, Xin-Lu Ye <sup>2,†</sup>, Yu-Bo Wang <sup>1</sup>, Ming-Li Yue <sup>1</sup>, Ping Li <sup>1</sup>, Liu Yang <sup>1</sup>, Yu-Long Liu <sup>1</sup>  and Ying Fu <sup>1,\*</sup> 

<sup>1</sup> Department of Chemistry, College of Arts and Sciences, Northeast Agricultural University, Harbin 150030, China; sunfangsunxue@163.com (F.S.); wangyubo970629@163.com (Y.-B.W.); yueml@neau.edu.cn (M.-L.Y.); liping198904@163.com (P.L.); yangliu@neau.edu.cn (L.Y.); liuyulong@neau.edu.cn (Y.-L.L.)

<sup>2</sup> Department of Applied Biology and Chemical Technology, Hong Kong Polytechnic University, Hung Hom, Hong Kong, China; 18082612d@connect.polyu.hk

\* Correspondence: fuying@neau.edu.cn

† These authors contributed equally to this work.

**Abstract:** Glyphosate is a highly effective, low-toxicity, broad-spectrum herbicide, which is extensively used in global agriculture to control weeds and vegetation. However, glyphosate has become a potential threat to human and ecosystem because of its excessive usage and its bio-concentration in soil and water. Herein, a novel turn-on fluorescent probe, N-n-butyl-4-(3-pyridinyl)methylidenehydrazine-1,8-naphthalimide (NPA), is proposed. It efficiently detected Cu<sup>2+</sup> within the limit of detection (LOD) of 0.21 μM and displayed a dramatic turn-off fluorescence response in CH<sub>3</sub>CN. NPA-Cu<sup>2+</sup> complex was employed to selectively and sensitively monitor glyphosate concentrations in real samples accompanied by a fluorescence turn-on mode. A good linear relationship between NPA and Cu<sup>2+</sup> of glyphosate was found in the range of 10–100 μM with an LOD of 1.87 μM. Glyphosate exhibited a stronger chelation with Cu<sup>2+</sup> than NPA and the system released free NPA through competitive coordination. The proposed method demonstrates great potential in quantitatively detecting glyphosate in tap water, local water from Songhua River, soil, rice, millet, maize, soybean, mung bean, and milk with mild conditions, and is a simple procedure with obvious consequences and no need for large instruments or pretreatment.

**Keywords:** fluorescent sensor; NPA-Cu<sup>2+</sup>; glyphosate; coordination competition; off-on



**Citation:** Sun, F.; Ye, X.-L.; Wang, Y.-B.; Yue, M.-L.; Li, P.; Yang, L.; Liu, Y.-L.; Fu, Y. NPA-Cu<sup>2+</sup> Complex as a Fluorescent Sensing Platform for the Selective and Sensitive Detection of Glyphosate. *Int. J. Mol. Sci.* **2021**, *22*, 9816. <https://doi.org/10.3390/ijms22189816>

Academic Editor: Wojciech Bal

Received: 23 August 2021

Accepted: 6 September 2021

Published: 10 September 2021

**Publisher's Note:** MDPI stays neutral with regard to jurisdictional claims in published maps and institutional affiliations.



**Copyright:** © 2021 by the authors. Licensee MDPI, Basel, Switzerland. This article is an open access article distributed under the terms and conditions of the Creative Commons Attribution (CC BY) license (<https://creativecommons.org/licenses/by/4.0/>).

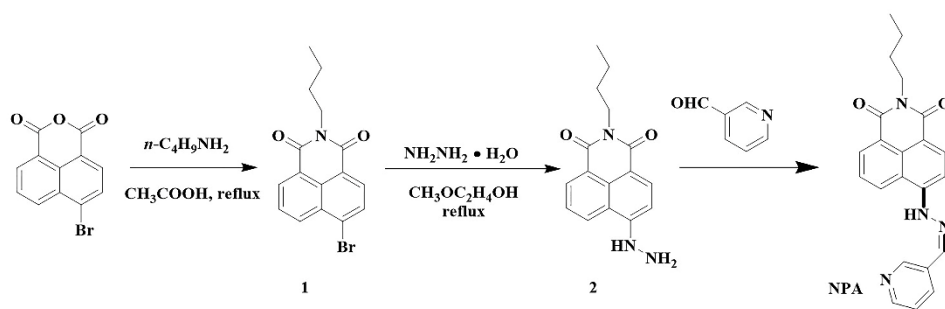
## 1. Introduction

Glyphosate (*N*-(phosphonomethyl) glycine) is an efficient, low-toxicity, and nonselective herbicide against perennial weeds [1]. It is widely used in economic crops or trees such as orchards, rice, maize, soybeans, wheat, and tea fields [2–4]. However, glyphosate has become a risk to human health because of its improper treatment and its bioconcentration in soil and water [5]. Glyphosate is a potential endocrine disruptor and exhibits adverse effects on cell cycle regulation [6,7]. It is classified as a potential carcinogen and genotoxic to humans by the International Agency for Research on Cancer (IARC) [8]. The U.S. Environmental Protection Agency set a maximum concentration of 700 μg/L for glyphosate in water [9]. Guidelines for Canadian Drinking Water Quality prescribe a limit of 280 μg/L in drinking water [10]. Therefore, establishing a convenient and reliable method for the accurate and rapid detection of glyphosate is necessary and of great urgency.

Several effective analytical strategies have been established for the detection of glyphosate. Traditional methods depend on expensive large-scale equipment, such as gas chromatography (GC), GC coupled with mass spectrometry (GC-MS), and high performance liquid chromatography (HPLC) [11,12]. To overcome the limitations of expensive instruments, tedious pretreatments, and derivatization procedures, several techniques have been proposed, such as enzyme-linked immunosorbent assay (ELISA) [13], capillary electrophoresis (CE) [14], amperometry [15], colorimetric assay [16], fluorescence spectrometry,

and electrochemical sensing [17,18]. These analytical techniques overcome the disadvantages of traditional methods to a certain extent; however, there are still some limitations. For example, ELISA utilizes expensive antibodies that are sensitive to temperature and pH, and electrochemical assays generally have short life cycles. Colorimetry is obvious; however, lacks good accuracy. Hence, it is critical to develop a facile, rapid, sensitive, and efficient method to detect glyphosate in environmental samples.

Recently, fluorescence detection for glyphosate has attracted much attention because of its easy operation, rapid response, high sensitivity, etc. Fluorescence sensors such as nanoclusters [19–21], quantum dots [22–24], and metal-organic frameworks have been used to detect glyphosate [25]. Currently, copper ion complexes are widely used due to their novelty, sensitivity, low toxicity, and membrane permeability [26–28]. A coumarin derivative and  $\text{Cu}^{2+}$  complex system was developed that selectively detected glyphosate with a good linear relationship of 0.02–1.50  $\mu\text{g}/\text{mL}$  [29]. Inspired by the designs of copper complexes and our continuous interest in pesticide identification [30–34], a new probe for  $\text{Cu}^{2+}$ , *N*-*n*-butyl-4-(3-pyridinyl)methylidenehydrazine-1,8-naphthalimide (**NPA**), was designed and synthesized (Scheme 1). **NPA** exhibited fluorescence quenching in the presence of  $\text{Cu}^{2+}$ . When glyphosate was added to the **NPA**- $\text{Cu}^{2+}$  system, the fluorescence was discovered with a color change from colorless to green. **NPA**- $\text{Cu}^{2+}$  can be used for ultra-sensitive detection of glyphosate in environmental samples with high sensitivity, fast response, and obvious consequences.



**Scheme 1.** Synthesis route to compound **NPA**.

## 2. Results

### 2.1. Spectral Characteristics of Probe **NPA** upon Coordination with $\text{Cu}^{2+}$

The solvent effects of **NPA** were studied in solvents of  $\text{CH}_3\text{CN}$ ,  $\text{CH}_3\text{CH}_2\text{OH}$ ,  $\text{DMSO}$ ,  $\text{DMF}$ , and  $\text{CH}_3\text{OH}$ , and  $\text{CH}_3\text{CN}$  was selected as the test solvent (Figure S4).

The responses of **NPA** were examined to evaluate the sensing properties with the introduction of other different metal ions. The UV–vis absorption spectrum of free **NPA** showed a maximum peak at 440 nm. The absorbance intensity of **NPA** decreased, accompanied by the yellow solution of **NPA** changing to colorless after the addition of  $\text{Cu}^{2+}$ , while the UV–vis spectra of other metal ions basically did not change, which indicated that **NPA** could serve as a highly selective “naked-eye” probe for  $\text{Cu}^{2+}$  (Figure 1a). The introduction of  $\text{Cu}^{2+}$  into the solution of **NPA** also caused significant fluorescence quenching (Figure 1b). Free **NPA** exhibited strong fluorescence with emission at 533 nm. The fluorescence intensity decreased quickly and was quenched with  $\text{Cu}^{2+}$  added after 100 s, after which the system color changed from green to colorless (Figure S5).

To further explore the characteristics of **NPA** for  $\text{Cu}^{2+}$ , competition and reversibility experiments were carried out. The fluorescence intensity of the **NPA**- $\text{Cu}^{2+}$  system was slightly enhanced after  $\text{Al}^{3+}$  was added, and the introduction of other interference metal ions did not affect the detection of  $\text{Cu}^{2+}$  by **NPA** (Figure S6). Alternating additions of  $\text{Cu}^{2+}$  and EDTA to the system caused variation in the fluorescence intensity (Figure S7). Although a certain degree of decrease in the fluorescence intensity was found after several cycles, **NPA** showed good reversibility. The results indicate that **NPA** could serve as a specific, rapid, and reversible sensor for  $\text{Cu}^{2+}$  detection.

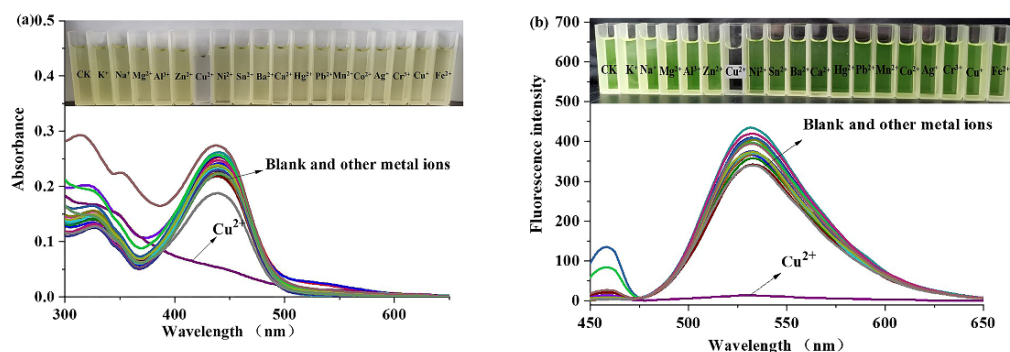


**Figure 1.** UV-vis (a) and fluorescence (b) spectra of **NPA** toward various metal cations.

The fluorescence intensity of **NPA** was recorded at various concentrations of  $\text{Cu}^{2+}$  in  $\text{CH}_3\text{CN}$  for quantitative analysis. The fluorescence intensity decreased gradually with increasing the  $\text{Cu}^{2+}$  concentration from 0 to 1.9 eq. and remained stable after 1.9 eq.  $\text{Cu}^{2+}$  was added (Figure 2a). A desirable linear relationship was observed between the fluorescence intensity and  $\text{Cu}^{2+}$  concentration, represented by  $y = -21.20x + 376.29$  ( $R^2 = 0.99$ ) (Figure 2b). The binding constant ( $K_{11}$ ) was calculated to be  $1.8 \times 10^4 \text{ M}^{-1}$  (Figure S8), which was calculated with validated open-source software (BindFit) [35]. The limit of detection (LOD) for  $\text{Cu}^{2+}$  was calculated to be  $0.21 \mu\text{M}$  based on the equation of  $\text{LOD} = 3\sigma/k$ , where  $\sigma$  is the blank standard deviation and  $k$  is the slope of the fluorescence intensity ratio vs. analyte concentration plot [36]. Comparing with **NPA** and other  $\text{Cu}^{2+}$  sensors based on Schiff's base with different sensing mechanisms (Table S1), the LOD of **NPA** was low enough to detect  $\text{Cu}^{2+}$ .

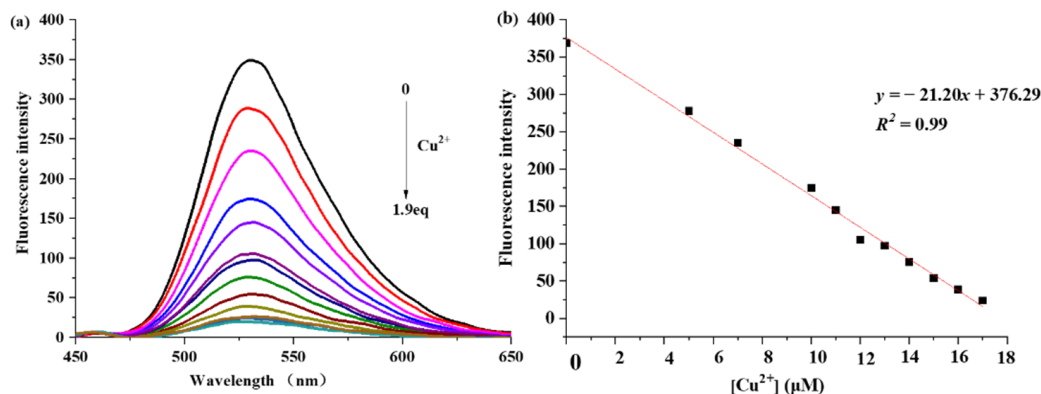


**Figure 2.** (a) Fluorescence spectrum of **NPA** on the addition of different amounts of  $\text{Cu}^{2+}$  in a  $\text{CH}_3\text{CN}$  solution; (b) the linear responses of **NPA** with  $\text{Cu}^{2+}$  concentrations.

To determine the stoichiometric ratio of **NPA** binding to  $\text{Cu}^{2+}$ , a Job's plot was constructed (Figure 3). The maximum fluorescence change was observed at a mole fraction of 0.65, indicating a 2:1 binding mode of **NPA** and  $\text{Cu}^{2+}$ .

The IR and NMR spectra of **NPA-Cu**<sup>2+</sup> were employed to elucidate the sensing mechanism. The IR spectroscopic comparison is shown in Figures 4 and 5. These results further confirm that NH participated in the complex leading to a reverse photoinduced electron transfer (PET) process and resulted in fluorescence quenching (Scheme 2).

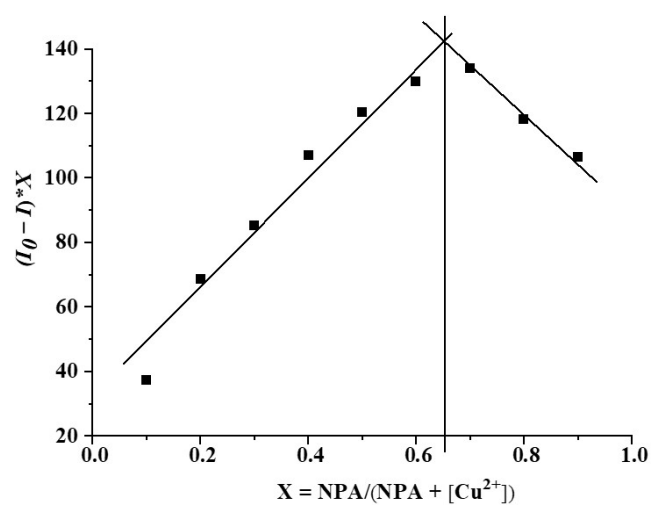


Figure 3. Job's plot for the binding ratio between NPA and  $\text{Cu}^{2+}$ .

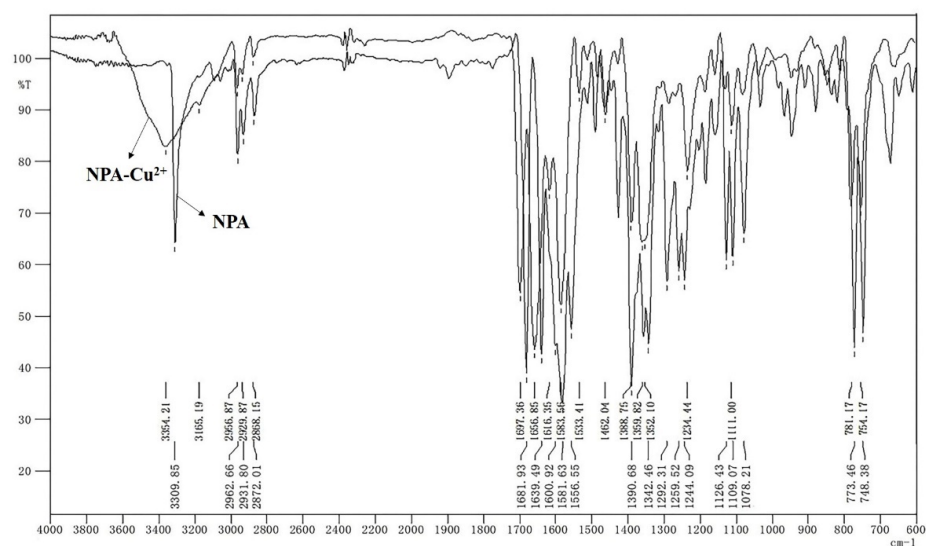


Figure 4. The FT-IR spectra of NPA compound before and after the introduction of  $\text{Cu}^{2+}$ .

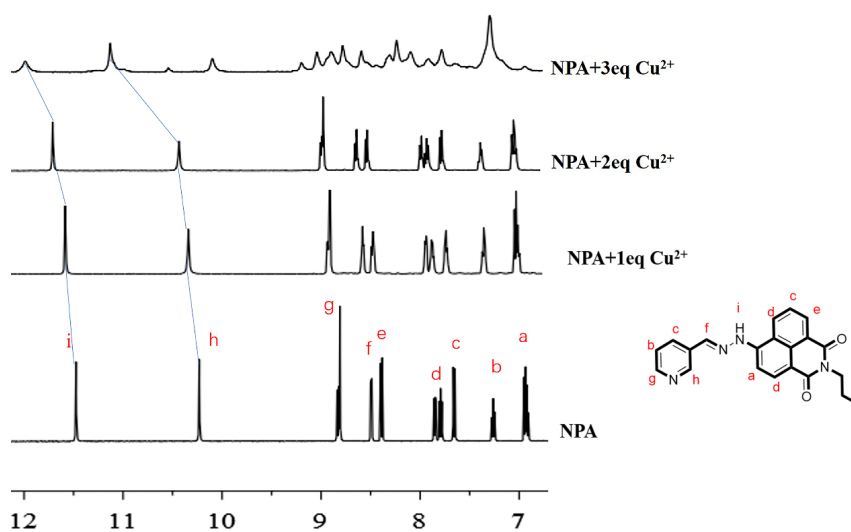
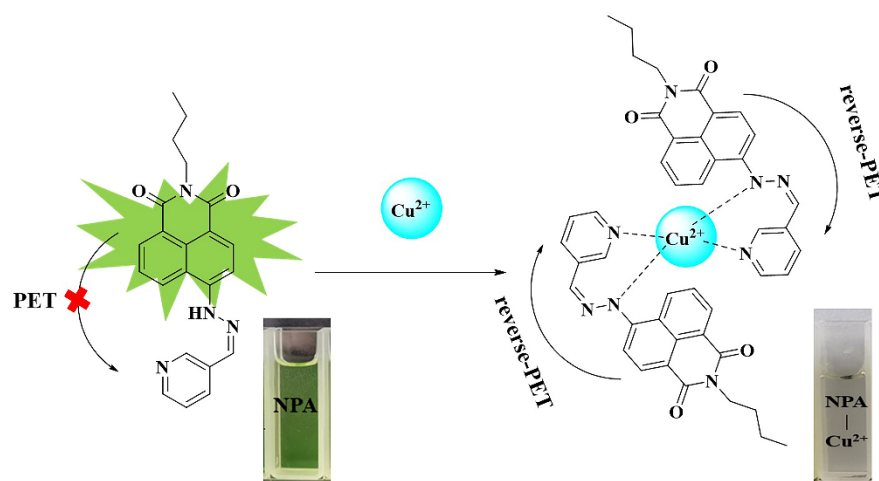
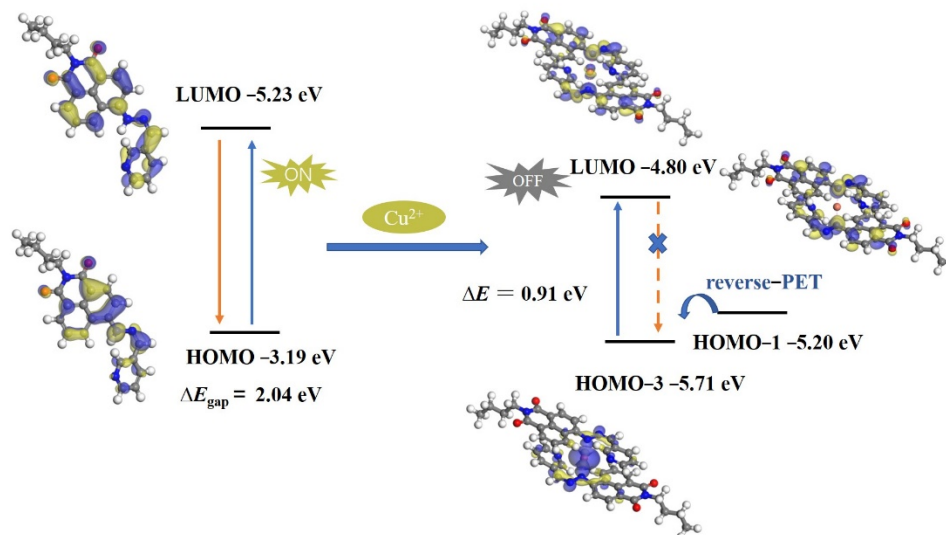


Figure 5.  $^1\text{H}$  NMR titration plots of NPA probe with  $\text{Cu}^{2+}$  in  $\text{DMSO}-d_6$ . (a, c, d, e: naphthalimide; b, c, g, h: pyridine; f: CH-N; i: NH).



**Scheme 2.** Possible sensing mechanism of NPA and  $\text{Cu}^{2+}$ .

To further explore the changes in NPA and  $\text{Cu}^{2+}$  before and after coordination, the frontier orbital energy diagram of NPA and  $\text{NPA-Cu}^{2+}$  from the PBE was constructed using DFT (Figure 6). Electrons of the fluorophore in NPA transferred from its HOMO to the LUMO and then returned to its HOMO without passing through the HOMO of the receptor in NPA, causing the free probe NPA to exhibit a fluorescence when on. When  $\text{Cu}^{2+}$  was added, the  $\Delta E$  of the system decreased, and the electrons were transferred from the 1,8-naphthalimide moiety (HOMO-1) to the electrondeficient pyridine groups (HOMO-3). These results demonstrate that the quenching response of NPA to  $\text{Cu}^{2+}$  ions could be considered a reverse PET process [37–39].

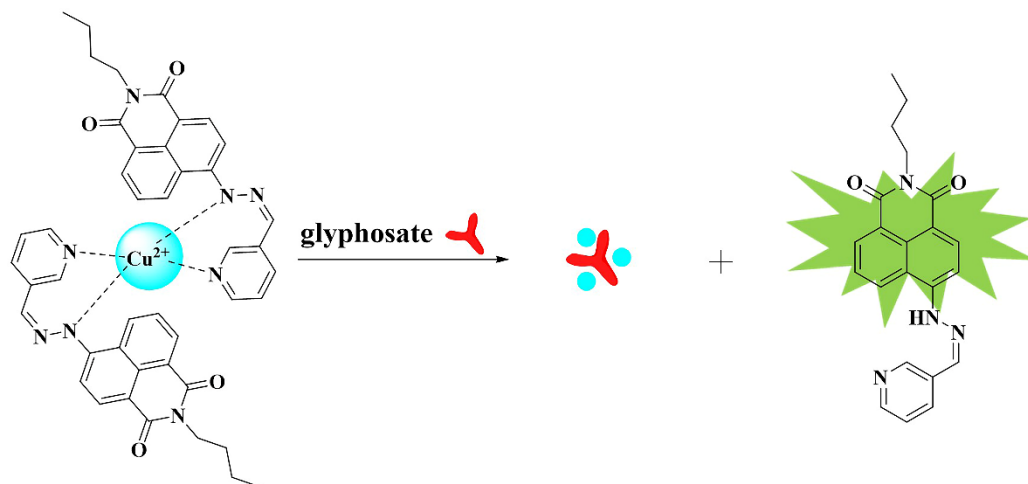


**Figure 6.** Frontier orbital energy diagram and electron transfer path in NPA and  $\text{NPA-Cu}^{2+}$ .

## 2.2. Sensing Assay for Glyphosate by $\text{NPA-Cu}^{2+}$

The binding mode between glyphosate and  $\text{Cu}^{2+}$  has been confirmed by EXAFS spectra [40,41].  $\text{Cu}^{2+}$  ions lie at the center of a Jahn-Teller distorted octahedron with the amine, carboxylate, and phosphonate groups of glyphosate chelating with  $\text{Cu}^{2+}$  to form two five-membered chelate rings oriented in the equatorial plane. A sensing approach for glyphosate was developed, inspired by the aforementioned mechanism via competitive coordination between the  $\text{NPA-Cu}^{2+}$  complex and glyphosate, as shown in Scheme 3. When glyphosate is present in the  $\text{NPA-Cu}^{2+}$  system, the functional groups of glyphosate, such as carboxylate, amine, and phosphonate, chelated with  $\text{Cu}^{2+}$  to form the more stable

complex, in order to release the NPA, and the fluorescence intensity of the system can recover. Therefore, it is feasible in theory to regard the competitive coordination balance between  $\text{NPA-Cu}^{2+}$  and glyphosate as a new method for the detection of glyphosate residue.



**Scheme 3.** Proposed sensing mechanism of  $\text{NPA-Cu}^{2+}$  and glyphosate.

The fluorescence intensity gradually increased with increasing glyphosate concentration in the  $\text{NPA-Cu}^{2+}$  system (Figure 7a). The fluorescence response versus the concentrations of glyphosate showed a desirable linear relationship in the concentration range of 0 to 11 eq., as described by the linear equation  $y = 2.40x + 34.53$ , with a linear coefficient of 0.99 (Figure 7b). The binding constant ( $K_{11}$ ) was calculated as  $K_{11} = 9.6 \times 10^4 \text{ M}^{-1}$ , according to Host-Guest interaction BindFit (Figure S9). The LOD was calculated to be  $1.87 \mu\text{M}$  ( $0.32 \mu\text{g/mL}$ ).

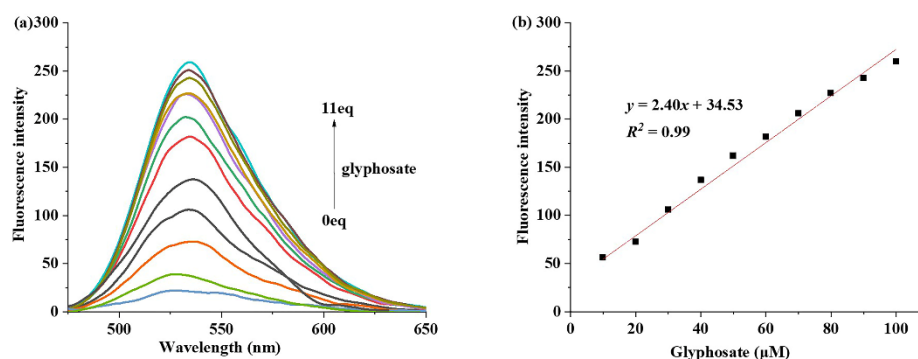


**Figure 7.** (a) Fluorescence spectrum of  $\text{NPA-Cu}^{2+}$  on the addition of different amount of glyphosate in a  $\text{CH}_3\text{CN}$  solution; (b) the linear responses of  $\text{NPA-Cu}^{2+}$  with glyphosate concentrations.

To evaluate the specificity of the  $\text{NPA-Cu}^{2+}$  system to glyphosate, selective and inter-ferential tests were conducted. Some typical organophosphorus pesticides were selected, such as glufosinate, trichlorfon, phosethy-Al, trichlorfon, and fosthiazate. In addition, the triketone herbicide mesotrione, the fluorine-containing pesticide oxyfluorfen, and common everyday ligands (alanine and serine) were selected as negative interferences (Scheme 4). As shown in Figure 8a, after introducing glyphosate to the  $\text{NPA-Cu}^{2+}$  system, the fluorescence intensity of the system increased significantly. When glufosinate, alanine, and serine were added, the fluorescence intensity of the system slightly increased, while the other pesticides did not affect the chelation (Figure 8b).

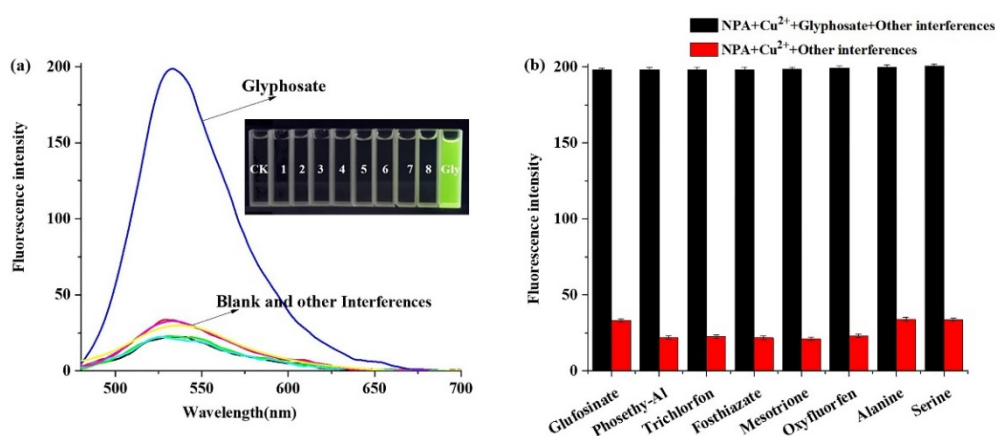
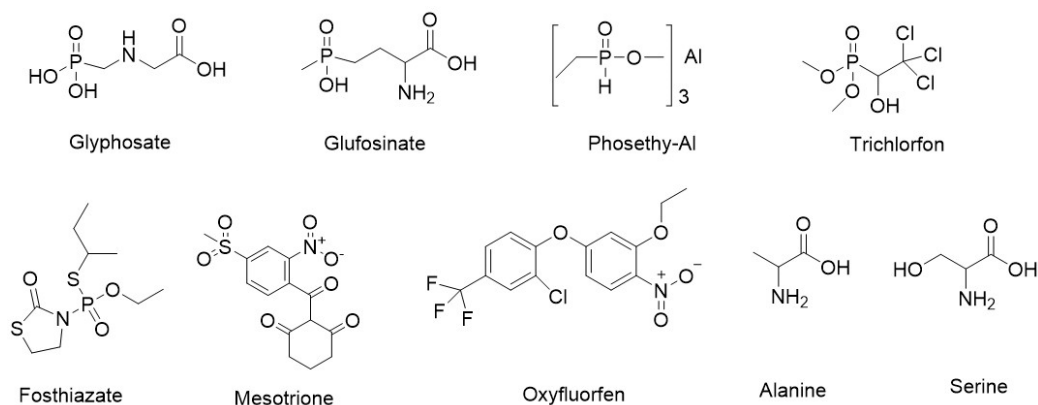


**Figure 8.** (a) Fluorescence spectral changes in  $\text{NPA-Cu}^{2+}$  toward various pesticides (Gly: glyphosate); (b) fluorescence response of  $\text{NPA-Cu}^{2+}$  upon the addition of various pesticides.

Other pesticides did not interfere with  $\text{NPA-Cu}^{2+}$  system, and glyphosate was quickly and specifically recognized within 300 s (Figure S10). All of these results indicate that  $\text{NPA-Cu}^{2+}$  detects glyphosate specifically and quickly, and is valuable in monitoring glyphosate in real time.

### 2.3. Applications in Real Samples

To explore the practicality of the  $\text{NPA-Cu}^{2+}$  system, tap water, local water from Songhua River, soil collected from the Northeast Agricultural University campus (Harbin, China), rice, millet, maize, soybean, mung bean, and milk directly purchased from local supermarkets were used for comparison. Different concentrations (30, 60, and 90  $\mu\text{M}$ ) of glyphosate standard solutions were added to these samples and detected through the  $\text{NPA-Cu}^{2+}$  system. Satisfactory fortified recoveries of 98.8–116.7% were obtained, and the relative standard deviations were all less than 2.5% (Table 1). Compared with previously reported sensing systems for glyphosate (Table 2), this strategy is more sensitive than others, and features no enzymatic mild conditions, has no need for large instruments or pretreatment, but has a simple procedure with obvious consequences [42–45]. The results indicate that the sensor system possesses significant potential for practical applications related to the environmental monitoring of glyphosate.

**Table 1.** Detection of glyphosate in water samples and soil samples using the proposed method.

Samples	Added ( $\mu\text{M}$ )	Found ( $n = 3$ ) ( $\mu\text{M}$ )	Recovery ( $n = 3$ ) (%)	RSD (%)
Soil	-	$0.0 \pm 0.0$	-	-
	30	$34.5 \pm 0.1$	$115.0 \pm 1.7$	1.9
	60	$62.9 \pm 0.2$	$104.8 \pm 0.4$	1.2
	90	$93.6 \pm 0.1$	$104.0 \pm 0.1$	2.0
Songhua River	-	$0.0 \pm 0.0$	-	-
	30	$35.2 \pm 0.3$	$116.7 \pm 0.2$	2.5
	60	$66.0 \pm 0.1$	$110.3 \pm 0.1$	1.5
	90	$94.1 \pm 0.6$	$104.4 \pm 1.1$	0.9
Tap Water	-	$0.0 \pm 0.0$	-	-
	30	$33.2 \pm 0.2$	$109.6 \pm 1.1$	1.6
	60	$65.4 \pm 0.4$	$105.6 \pm 0.1$	1.4
	90	$89.3 \pm 0.5$	$98.8 \pm 0.1$	2.1
Rice	-	$0.0 \pm 0.0$	-	-
	30	$32.5 \pm 0.1$	$108.3 \pm 0.8$	1.5
	60	$62.8 \pm 0.3$	$104.6 \pm 0.3$	2.3
	90	$89.5 \pm 0.5$	$99.4 \pm 0.5$	1.8
Milk	-	$0.0 \pm 0.0$	-	-
	30	$31.9 \pm 0.3$	$106.3 \pm 1.3$	1.6
	60	$61.7 \pm 0.5$	$102.8 \pm 1.5$	1.1
	90	$89.8 \pm 0.6$	$99.7 \pm 0.8$	2.3
Millet	-	$0.0 \pm 0.0$	-	-
	30	$31.5 \pm 0.9$	$105.0 \pm 0.3$	0.9
	60	$61.4 \pm 0.7$	$102.5 \pm 0.1$	0.5
	90	$90.6 \pm 0.9$	$100.7 \pm 0.1$	0.7
Maize	-	$0.0 \pm 0.0$	-	-
	30	$30.7 \pm 0.3$	$102.3 \pm 0.3$	0.7
	60	$60.7 \pm 0.2$	$101.2 \pm 0.1$	0.5
	90	$90.5 \pm 0.3$	$105.5 \pm 0.1$	0.7
Soybean	-	$0.0 \pm 0.0$	-	-
	30	$30.6 \pm 0.2$	$102.3 \pm 0.3$	0.9
	60	$60.8 \pm 0.4$	$101.5 \pm 0.5$	1.0
	90	$90.2 \pm 0.3$	$100.5 \pm 0.6$	1.8
Mung bean	-	$0.0 \pm 0.0$	-	-
	30	$29.0 \pm 0.4$	$96.6 \pm 0.1$	0.4
	60	$59.2 \pm 0.3$	$98.6 \pm 0.6$	0.5
	90	$89.4 \pm 0.2$	$99.3 \pm 0.3$	0.3

**Table 2.** Comparison of different strategies to detect glyphosate.

Sensing System	Range ( $\mu\text{g/mL}$ )	LOD ( $\mu\text{g/mL}$ )	Application	Reference
CDs- $\text{Fe}^{3+}$	0.1–16	8.75	Potatoes	[22]
Gold Electrode	50–300	2.0	Water	[42]
LC-MS/MS	1–250	0.5	Serum	[43]
Electrochemical sensor	1.7–16.9	0.98	Soil	[44]
Capillary electrophoretic methodologies	1.0–8.0	0.5	Water	[45]
NPA- $\text{Cu}^{2+}$	0–18.6	0.32	Water Soil	This work

### 3. Discussion

#### 3.1. Sensing Mechanism of $\text{Cu}^{2+}$ by NPA

There was a sharp peak at around  $3309 \text{ cm}^{-1}$  in the IR spectra of NPA, which could be assigned to the NH of the hydrazine group. This peak was replaced by a broad peak at  $3358 \text{ cm}^{-1}$  in the complex (NPA- $\text{Cu}^{2+}$ ) spectrum, indicating the involvement of NH

in the complexation. To further investigate the binding site of NPA with  $\text{Cu}^{2+}$ ,  $^1\text{H}$  NMR titrations were carried out. The obvious change was that the proton signal (site i) of the NH gradually decreased with the addition of  $\text{Cu}^{2+}$ , while the proton signal of the =CH– group in the pyridine ring at 10.23 ppm (site h) gradually shifted to the lower field due to the paramagnetic properties of  $\text{Cu}^{2+}$ . When 3 eq.  $\text{Cu}^{2+}$  was added, the proton signal of the NH almost disappeared and the proton signal of the =CH– group in the pyridine ring moved to 10.85 ppm. These further confirm that NH participated in the complex leading to a reverse photoinduced electron transfer (PET) process and resulted in fluorescence quenching [46–48].

### 3.2. Sensing Mechanism of Glyphosate by NPA- $\text{Cu}^{2+}$

The experimental result that the NPA- $\text{Cu}^{2+}$  complex system can specifically recognize glyphosate is attributed to the relative spatial proximity of the phosphonate amino and carboxyl groups of glyphosate to each other, facilitating the formation of chelates with  $\text{Cu}^{2+}$ . Although glufosinate and glyphosate are similar in structure, the amino and phosphonate groups are separated by three methylenes in glufosinate, which make it difficult to form a steric chelation with  $\text{Cu}^{2+}$ . Alanine and serine are structurally similar to glufosinate, and cannot form a stable steric chelation with  $\text{Cu}^{2+}$ . However, other similar pesticides lacking coordination groups failed to form stable coordinations with  $\text{Cu}^{2+}$ , and could not form chelations in space.

## 4. Materials and Methods

### 4.1. Materials and Physical Instruments

All analytical reagent-grade chemicals and solvents employed for the experiment, which were purchased from commercial providers, were used without further purification. Glyphosate, glufosinate, trichlorfon, phosethy–Al, fosthiazate, mesotrione, and oxyfluorfen were purchased from Altai Biological Technology Co., Ltd. (Hebei, China).

FT–IR spectra were measured on a Bruker ALPHA–T spectrometer, which used KBr pellets with a range of 4000–600  $\text{cm}^{-1}$  (Bruker Corp., Billerica, MA, USA). The  $^1\text{H}$  and  $^{13}\text{C}$  NMR spectra were recorded on a Bruker AV400 NMR spectrometer by using  $\text{DMSO-}d_6$  as the solvent, and the chemical shifts are reported in ppm (Bruker Corp., Billerica, MA, USA). The HRMS was obtained on an FTMS Ultral Apex MS spectrometer (Bruker Corp., Billerica, MA, USA). The absorption spectra were gained on a Shimadzu UV-2700 UV–vis spectrometer at 25 °C (Shimadzu Corp., Kyoto, Japan). Fluorescence spectra were obtained on a PerkinElmer LS55 fluorescence spectrometer (PerkinElmer Corp., Waltham, MA, USA) with a xenon lamp and quartz carrier.

### 4.2. Synthesis of the Probe NPA

N-n-butyl-4-bromo-1,8-naphthalimide (1) and N-n-butyl-4-hydrazine hydrate-1,8-naphthalic anhydride (2) were synthesized according to previous research of our group [49–51]. Compound 2 (283.0 mg, 1 mmol) and  $\beta$ -nicotinaldehyde (40%, w/w, 3.0 mL) were added to EtOH (20 mL). The mixture was refluxed for 2 h and then cooled to room temperature. The precipitate was filtered and washed with EtOH to obtain an orange solid with a yield of 66%. IR (KBr,  $\nu$ ,  $\text{cm}^{-1}$ ) 3309(N–H), 2957, 2858(C–H), 1635(C=O), 1126(C–N).  $^1\text{H}$  NMR (400 MHz,  $\text{DMSO-}d_6$ )  $\delta$  11.48 (s, 1H), 10.23 (s, 1H), 8.82 (d, J = 5.9 Hz, 1H), 8.49 (d, J = 7.3 Hz, 1H), 8.39 (d, J = 8.5 Hz, 1H), 7.85 (d, J = 7.8 Hz, 1H), 7.82–7.77 (m, 1H), 7.66 (d, J = 8.5 Hz, 1H), 7.26 (t, J = 7.7 Hz, 1H), 6.96–6.90 (m, 2H), 4.06–4.01 (m, 2H), 1.65–1.57 (m, 2H), 1.35 (m, J = 7.4 Hz, 2H), 0.93 (t, J = 7.4 Hz, 3H).  $^{13}\text{C}$  NMR (100 MHz,  $\text{DMSO-}d_6$ )  $\delta$  164.02, 163.36, 149.94, 148.27, 146.53, 140.92, 134.01, 133.69, 131.31, 131.22, 129.45, 128.61, 125.50, 124.62, 122.46, 119.13, 112.00, 107.65, 40.02, 30.23, 20.31, 14.19. HRMS (ESI): calculated for  $\text{C}_{22}\text{H}_{20}\text{N}_4\text{O}_2$  [M + H] $^+$  373.1658, obtained a value of 373.1659.

The original spectra of NPA are included in the electronic Supplementary Information (Figures S1–S3).

#### 4.3. General Procedures for Spectrophotometric Studies

The solvent effects of **NPA** ( $10^{-5}$  M) were studied in the solvents of  $\text{CH}_3\text{CN}$ ,  $\text{CH}_3\text{CH}_2\text{OH}$ , DMSO, DMF, and  $\text{CH}_3\text{OH}$ , and then  $\text{CH}_3\text{CN}$  was selected as the solvent to be tested. The stock solutions of  $10^{-2}$  M metal ions were provided from NaCl, KCl, CuCl, AgNO<sub>3</sub>, CuCl<sub>2</sub>, MgCl<sub>2</sub>, NiCl<sub>2</sub>, ZnCl<sub>2</sub>, SnCl<sub>2</sub>, BaCl<sub>2</sub>, MnCl<sub>2</sub>, CaCl<sub>2</sub>, HgCl<sub>2</sub>, PbCl<sub>2</sub>, BaCl<sub>2</sub>, CoCl<sub>2</sub>, HgCl<sub>2</sub>, PbCl<sub>2</sub>, FeCl<sub>2</sub>, AlCl<sub>3</sub>, and CrCl<sub>3</sub> using ultrapure water. A  $\text{Cu}^{2+}$  solution (1 mL,  $10^{-2}$  M) was added to a 10 mL volumetric flask and diluted to  $10^{-3}$  M in ultrapure water. **NPA** ( $10^{-5}$  M) solutions of 9.0, 8.0, 7.0, 6.0, 5.0, 4.0, 3.0, 2.0, and 1.0 mL were taken and transferred to 10.0 mL volumetric flasks.  $\text{Cu}^{2+}$  ( $10^{-3}$  M) solutions of 10, 20, 30, 40, 50, 60, 70, 80, and 90  $\mu\text{L}$  were added to each **NPA** solution, so that the mole fractions of **NPA** became 0.1, 0.2, 0.3, 0.4, 0.5, 0.6, 0.7, 0.8, and 0.9, respectively. Each bottle was diluted with  $\text{CH}_3\text{CN}$  to 10 mL [52]. Ethylene diamine tetraacetic acid (EDTA) solution ( $10^{-2}$  M) for a reversible experiment was obtained with ultrapure water.

#### 4.4. Theoretical Calculation Methods

The quantum chemical calculations of the optimized structures were conducted by applying density functional theory (DFT) in Material Studio. The structure was optimized using the Perdew-Burke-Ernzerh (PBE) method of generalized gradient approximation (GGA) in the Dmol3 module for **NPA** and a model **NPA-Cu<sup>2+</sup>** complex.

#### 4.5. Measurement of Glyphosate Using the **NPA-Cu<sup>2+</sup>** System

An **NPA** solution (10.0 mL,  $10^{-4}$  M) and a  $\text{Cu}^{2+}$  aqueous solution (200  $\mu\text{L}$ ,  $10^{-2}$  M) were added to a 100 mL volumetric flask, and then the volume was fixed with  $\text{CH}_3\text{CN}$  to configure the **NPA-Cu<sup>2+</sup>** solution ( $10^{-5}$  M). Subsequently, the final mixture was incubated for 5 min at 30 °C, and the fluorescence intensity at 533 nm was recorded with  $\lambda_{\text{ex}}$  at 440 nm. Interference (glyphosate, glufosinate, trichlorfon, phosethy-Al, fosthiazate, mesotrione, oxyfluorfen, alanine, and serine) solutions ( $10^{-2}$  M) were prepared for interference and selective experiments.

#### 4.6. Applications in Real Samples

In order to verify the practical applications, tap water, local water from Songhua River, and soil collected from the Northeast Agricultural University campus (Harbin, China), rice, millet, maize, soybean, mung bean, and milk purchased directly from the local supermarkets were selected as the real samples and were tested by the proposed sensor through the standard addition method. Water from Songhua River was filtered through a 0.22  $\mu\text{m}$  membrane to remove large solids and most impurities. The rice, millet, maize, soybean, and mung bean samples were ground into powders. Soil and rice millet, maize, soybean, and mung bean samples (10 g) were dispersed in 100 mL deionized water under ultrasonication for 15 min, centrifuged at 5000 rpm for 10 min, and then filtered through a 0.22  $\mu\text{m}$  microporous membrane for subsequent analyses [40,53]. Additionally, different concentrations (30, 60, and 90  $\mu\text{M}$ ) of glyphosate standard solutions were added to these samples and detected through the **NPA-Cu<sup>2+</sup>** system.

### 5. Conclusions

In summary, a highly selective and sensitive naphthalimide-based derivative sensor **NPA** and a  $\text{Cu}^{2+}$  complex (**NPA-Cu<sup>2+</sup>** system) for glyphosate detection were established. **NPA** was synthesized as an indicator of  $\text{Cu}^{2+}$  with turn-off fluorescence through coordination, and the LOD for  $\text{Cu}^{2+}$  detection was found to be 0.21  $\mu\text{M}$ . The phosphonate, amino, and carboxyl groups of glyphosate are relatively close to each other, allowing a chelate to form, and thus the space cyclization to chelate with  $\text{Cu}^{2+}$ . When glyphosate was added to the **NPA-Cu<sup>2+</sup>** system, **NPA** was released within 300 s and the fluorescence showed a turn-on pattern with a detection limit of 1.87  $\mu\text{M}$  for glyphosate. Further study revealed that glyphosate was successfully detected in water, soil, rice, millet, maize, soybean, mung bean, and milk samples by the **NPA-Cu<sup>2+</sup>** system. Considering the merits of the **NPA-Cu<sup>2+</sup>**

system to detect glyphosate, namely it is rapid, sensitive mild, easy to operate, and does not require large-scale equipment, it is expected to become a potential method for the efficient detection of glyphosate.

**Supplementary Materials:** The following are available online at <https://www.mdpi.com/article/10.3390/ijms22189816/s1>.

**Author Contributions:** Y.F. conceived and designed the experiment and conveyed the manuscript information as corresponding authors. F.S. and X.-L.Y. repeated the experiment multiple times and then used it as content for in-depth research. F.S. and X.-L.Y. used Origin and Microsoft Excel to process the data. M.-L.Y. and Y.-B.W. performed theoretical calculations. P.L. coordinated all of the data. Y.-L.L. and L.Y. consulted related literature, collected background knowledge and provided theoretical support. F.S. and X.-L.Y. synthesized and purified the compound. F.S. wrote the manuscript, which was edited by Y.F. All authors have read and agreed to the published version of the manuscript.

**Funding:** The work was supported by the National Natural Science Foundation of China (No. 51903032), the Natural Science Foundation of Heilongjiang Province (No. LH2019B002), the Post-doctoral Science Foundation of Heilongjiang Province (No. LBH-Z19045), and the “Young Talents” Project of Northeast Agricultural University of Heilongjiang Province (No. 18QC64).

**Institutional Review Board Statement:** Not applicable.

**Informed Consent Statement:** Not applicable.

**Data Availability Statement:** Not applicable.

**Acknowledgments:** The authors thank Min Zhang (Northeast Normal University) for assistance with the DFT calculation and analysis.

**Conflicts of Interest:** The authors declare no conflict of interest.

## References

1. Qiao, C.K.; Wang, C.X.; Pang, R.L.; Tian, F.J.; Han, L.J.; Guo, L.L.; Fang, J.B. Environmental behavior and influencing factors of glyphosate in peach orchard ecosystem. *Ecotox. Environ. Safe* **2020**, *206*, 11209. [[CrossRef](#)]
2. Benbrook, C.M. Trends in glyphosate herbicide use in the United States and globally. *Environ. Sci. Eur.* **2016**, *28*, 3. [[CrossRef](#)]
3. Conrad, A.; Schroter-Kermani, C.; Hoppe, H.W.; Ruther, M.; Pieper, S.; Kolossa-Gehring, M. Glyphosate in German adults-time trend (2001 to 2015) of human exposure to a widely used herbicide. *Int. J. Hyg. Environ. Health* **2017**, *220*, 8–16. [[CrossRef](#)] [[PubMed](#)]
4. Duke, S.O. The history and current status of glyphosate. *Pest Manag. Sci.* **2018**, *74*, 1027–1034. [[CrossRef](#)] [[PubMed](#)]
5. Liu, Z.; Yang, L.; Sharma, A.S.; Chen, M.; Chen, Q. A system composed of polyethylenimine-capped upconversion nanoparticles, copper (II), hydrogen peroxide and 3,3',5,5'-tetramethylbenzidine for colorimetric and fluorometric determination of glyphosate. *Microchim. Acta* **2019**, *186*, 835. [[CrossRef](#)]
6. Gasnier, C.; Dumont, C.; Benachour, N.; Clair, E.; Chagnon, M.C.; Seralini, G.E. Glyphosate-based herbicides are toxic and endocrine disruptors in human cell lines. *Toxicology* **2009**, *262*, 184–191. [[CrossRef](#)] [[PubMed](#)]
7. Wozniak, E.; Reszka, E.; Jablonska, E.; Balcerczyk, A.; Broncel, M.; Bukowska, B. Glyphosate affects methylation in the promoter regions of selected tumor suppressors as well as expression of major cell cycle and apoptosis drivers in PBMCs (in vitro study). *Toxicol. In Vitro* **2020**, *63*, 104736. [[CrossRef](#)] [[PubMed](#)]
8. Guyton, K.Z.; Loomis, D.; Grosse, Y.; Grosse, F.E.; Benbrahim-Tallaa, L.; Guha, N.; Scoccianti, C.; Mattock, H.; Straif, K. Carcinogenicity of tetrachlorvinphos, parathion, malathion, diazinon, and glyphosate. *Lancet Oncol.* **2015**, *16*, 490–491. [[CrossRef](#)]
9. USEPA. *Edition of the Drinking Water Standards and Health Advisories*; United States Environmental Protection Agency: Washington, DC, USA, 2017.
10. Health Canada. Guidelines for canadian drinking water quality-supporting documents-glyphosate. In *Health Canada Guidelines*; Health Canada: Ottawa, ON, Canada, 1995.
11. Okada, E.; Coggan, T.; Anumol, T.; Clarke, B.; Allinson, G. A simple and rapid direct injection method for the determination of glyphosate and AMPA in environmental water samples. *Anal. Bioanal. Chem.* **2019**, *411*, 715–724. [[CrossRef](#)]
12. Islas, G.; Rodriguez, J.A.; Mendoza-Huizar, L.H.; Perez-Moreno, F.; Carrillo, E.G. Determination of glyphosate and aminomethyl phosphonic acid in soils by hplc with precolumn derivatization using 1,2-naphthoquinone-4-sulfonate. *J. Liq. Chromatogr. Relat. Technol.* **2014**, *37*, 1298–1309. [[CrossRef](#)]
13. Mortl, M.; Nemeth, G.; Juracsek, J.; Darvas, B.; Kamp, L.; Rubio, F.; Szekacs, A. Determination of glyphosate residues in Hungarian water samples by immunoassay. *Microchem. J.* **2013**, *107*, 143–151. [[CrossRef](#)]

14. Corbera, M.; Hidalgo, A.; Salvado, V.; Wieczorek, P. Determination of glyphosate and aminomethylphosphonic acid in natural water using the capillary electrophoresis combined with enrichment step. *Anal. Chim. Acta* **2005**, *54*, 3–7. [[CrossRef](#)]
15. Sanchez-Bayo, F.; Hyne, R.V.; Hyne, K.L. An amperometric method for the detection of amitrole, glyphosate and its aminomethylphosphonic acid metabolite in environmental waters using passive samplers. *Anal. Chim. Acta* **2010**, *675*, 125–131. [[CrossRef](#)]
16. Chen, Q.A.; Chen, H.; Li, Z.H.; Pang, J.; Lin, T.R.; Guo, L.Q.; Fu, F.F. Colorimetric sensing of glyphosate in environmental water based on peroxidase mimetic activity of MoS<sub>2</sub> nanosheets. *J. Nanosci. Nanotechnol.* **2017**, *17*, 5730–5734. [[CrossRef](#)]
17. Perez, A.L.; Tibaldo, G.; Sanchez, G.H.; Siano, G.G.; Marsili, N.R.; Schenone, A.V. A novel fluorimetric method for glyphosate and AMPA determination with NBD-Cl and MCR-ALS. *Spectrochim. Acta A* **2019**, *214*, 119–128. [[CrossRef](#)]
18. Aguirre, M.D.; Aguirre, S.E.; Gomez, C.G. A Cu<sup>2+</sup>-Cu/glassy carbon system for glyphosate determination. *Sensor. Actuat. B—Chem.* **2019**, *284*, 675–683. [[CrossRef](#)]
19. Hong, C.Y.; Ye, S.S.; Dai, C.Y.; Wu, C.Y.; Chen, L.L.; Huang, Z.Y. Sensitive and on-site detection of glyphosate based on papain-stabilized fluorescent gold nanoclusters. *Anal. Bioanal. Chem.* **2020**, *412*, 8177–8184. [[CrossRef](#)] [[PubMed](#)]
20. Jiang, M.D.; Chen, C.; He, J.B.; Zhang, H.Y.; Xu, Z.X. Fluorescence assay for three organophosphorus pesticides in agricultural products based on Magnetic-Assisted fluorescence labeling aptamer probe. *Food Chem.* **2020**, *307*, 125534. [[CrossRef](#)]
21. Wang, X.F.; Yang, Y.X.; Huo, D.Q.; Ji, Z.; Ma, Y.; Yang, M.; Luo, H.B.; Luo, X.G.; Hou, C.J.; Lv, J.Y. A turn-on fluorescent nanoprobe based on N-doped silicon quantum dots for rapid determination of glyphosate. *Microchimica. Acta* **2020**, *187*, 520–527. [[CrossRef](#)]
22. Hou, J.Z.; Wang, X.F.; Wang, S.Y.; Zhang, C.; Hou, C.J.; He, Q.; Huo, D.Q. A turn-on fluorescent sensor based on carbon dots from *Sophora japonica* leaves for the detection of glyphosate. *Anal. Methods* **2020**, *12*, 4130–4138. [[CrossRef](#)]
23. Bera, M.K.; Mohapatra, S. Ultrasensitive detection of glyphosate through effective photoelectron transfer between CdTe and chitosan derived carbon dot. *Colloid Surface A* **2020**, *596*, 124710. [[CrossRef](#)]
24. Yuan, J.; Jiang, S.; Liu, J.; Yang, H.; Zhang, Y.J.; Hu, X. Fluorescent carbon dots for glyphosate determination based on fluorescence resonance energy transfer and logic gate operation. *Sens. Actuat. B—Chem.* **2020**, *242*, 545–553. [[CrossRef](#)]
25. Chen, F.; Li, G.D.; Liu, H.; Leung, C.H.; Ma, D.L. G-quadruplex-based detection of glyphosate in complex biological systems by a time-resolved luminescent assay. *Sens. Actuat. B—Chem.* **2020**, *320*, 128393. [[CrossRef](#)]
26. Zhao, H.; Liu, X.F.; Ma, C.B. Sensitive Fluorescence Assay for the Detection of Alkaline Phosphatase Based on a Cu<sup>2+</sup>-Thiamine System. *Sensors* **2021**, *21*, 674. [[CrossRef](#)] [[PubMed](#)]
27. Padnya, P.; Shibaeva, K.; Arsenyev, M.; Baryshnikova, S.; Terenteva, O.; Shiabiev, I.; Khannanov, A.; Boldyrev, A.; Boldyrev, A.; Gerasimov, A.; et al. Catechol-containing schiff bases on thiacalixarene: Synthesis, copper (II) recognition, and formation of organic-inorganic copper-based materials. *Molecules* **2021**, *26*, 2334. [[CrossRef](#)] [[PubMed](#)]
28. Hao, H.; Zhao, C.; Zheng, L.; Zhang, X.J. Evaluation of fluorescent Cu<sup>2+</sup> probes: Instant sensing, cell permeable recognition and quantitative detection. *Molecules* **2021**, *26*, 512.
29. Wang, X.F.; Sakinati, M.; Yang, Y.X.; Ma, Y.; Yang, M.; Luo, H.B.; Hou, C.J.; Huo, D. The construction of a CND/Cu<sup>2+</sup> fluorescence sensing system for the ultrasensitive detection of glyphosate. *Anal. Methods-UK* **2020**, *12*, 520–527. [[CrossRef](#)]
30. Yang, L.; Liu, Y.L.; Liu, C.G.; Ye, F.; Fu, Y. Two luminescent dye@MOFs systems as dual-emitting platforms for efficient pesticides detection. *J. Hazard. Mater.* **2020**, *381*, 120966. [[CrossRef](#)]
31. Li, L.; Gao, S.; Yang, L.; Liu, Y.L.; Li, P.; Ye, F.; Fu, Y. Cobalt (II) complex as a fluorescent sensing platform for the selective and sensitive detection of triketone HPPD inhibitors. *J. Hazard. Mater.* **2021**, *404*, 124015. [[CrossRef](#)]
32. Wang, Z.W.; Zhao, L.X.; Ma, P.; Ye, T.; Fu, Y.; Ye, F. Fragments Recombination, Design, Synthesis, Safener Activity and CoMFA Model of Novel Substituted Dichloroacetylphenyl Sulfonamide Derivatives. *Pest Manag. Sci.* **2021**, *77*, 1724–1738. [[CrossRef](#)]
33. Ye, F.; Zhai, Y.; Guo, K.L.; Liu, Y.X.; Li, N.; Gao, S.; Zhao, L.X.; Fu, Y. Safeners improve maize tolerance under herbicide toxicity stress by increasing the activity of enzyme in vivo. *J. Agric. Food Chem.* **2019**, *67*, 11568–11576. [[CrossRef](#)] [[PubMed](#)]
34. Fu, Y.; Wang, M.; Zhao, L.X.; Zhang, S.Q.; Liu, Y.X.; Guo, Y.Y.; Zhang, D.; Gao, S.; Ye, F. Design, synthesis, herbicidal activity and CoMFA of novel aryl-formyl piperidinone HPPD inhibitors. *Pestic. Biochem. Physiol.* **2021**, *174*, 104811. [[CrossRef](#)]
35. Kampes, R.; Tepper, R.; Gorls, H.; Bellstedt, P.; Jager, M.; Schubert, U.S. Facile and Reliable Emission-Based Nanomolar Anion Sensing by Luminescent Iridium Receptors Featuring Chelating Halogen-Bonding Sites. *Chem. Eur. J.* **2020**, *26*, 14679–14687. [[CrossRef](#)] [[PubMed](#)]
36. Ye, F.; Liang, X.M.; Xu, K.X.; Pang, X.X.; Chai, Q.; Fu, Y. A novel dithiourea-appended naphthalimide “on–off” fluorescent probe for detecting Hg<sup>2+</sup> and Ag<sup>+</sup> and its application in cell imaging. *Talanta* **2019**, *200*, 494–502. [[CrossRef](#)] [[PubMed](#)]
37. Li, P.; Wang, Y. A new fluorescent sensor containing glutamic acid for Fe<sup>3+</sup> and its resulting complex as a secondary sensor for PPI in purely aqueous solution. *New. J. Chem.* **2017**, *41*, 4234–4240. [[CrossRef](#)]
38. Li, C.; Han, X.T.; Mao, S.S.; Aderinto, S.O.; Shi, X.K.; Shen, K.S.; Wu, H.L. A new, highly potent 1,8-naphthalimide-based fluorescence turn-off chemosensor capable of detecting Cu (II) ions in real-world water samples. *Color Technol.* **2018**, *134*, 230–239. [[CrossRef](#)]
39. Sun, X.; Liu, Y.R.; Niu, N.; Chen, L.G. Synthesis of molecularly imprinted fluorescent probe based on biomass-derived carbon quantum dots for detection of mesotrione. *Anal. Bioanal. Chem.* **2019**, *411*, 5519–5530. [[CrossRef](#)]
40. Wang, L.; Bi, Y.D.; Gao, J.; Li, Y.J.; Ding, H.; Ding, L. Carbon dots based turn-on fluorescent probes for the sensitive determination of glyphosate in environmental water samples. *RSC Adv.* **2016**, *89*, 85820–85828. [[CrossRef](#)]
41. Sheals, J.; Persson, P.; Hedman, B. IR and EXAFS spectroscopic studies of glyphosate protonation and copper (II) complexes of glyphosate in aqueous solution. *Inorg. Chem. Front.* **2001**, *40*, 4302–4309. [[CrossRef](#)]

42. Noori, J.S.; Dimaki, M.; Mortensen, J.; Svendsen, W.E. Detection of glyphosate in drinking water: A fast and direct detection method without sample pretreatment. *Sensors—Basel* **2018**, *18*, 2961. [[CrossRef](#)]
43. Saito, T.; Namera, A.; Tsuji, T.; Noguchi, W.; Inokuchi, S. Determination of glyphosate and glufosinate in human serum by monospin TiO extraction and liquid chromatography-tandem mass spectrometry. *Acta Chromatogr.* **2020**, *32*, 10–15. [[CrossRef](#)]
44. Mbokana, J.G.Y.; Dedzo, G.K.; Ngameni, E. Grafting of organophilic silane in the interlayer space of acid-treated smectite: Application to the direct electrochemical. *Appl. Clay Sci.* **2020**, *188*, 105513. [[CrossRef](#)]
45. Moraes, M.P.; Goncalves, L.M.; Pereira, E.A. Determination of glyphosate and aminomethylphosphonic acid by capillary electrophoresis with indirect detection using pyridine-2,6-dicarboxylic acid or 3,5-dinitrobenzoic acid. *Int. J. Environ. Anal. Chem.* **2018**, *98*, 258–270. [[CrossRef](#)]
46. Bao, Z.M.; Qin, C.X.; Wang, J.J.; Sun, J.; Dai, L.X.; Chen, G.Q.; Mei, F. Sensitive and selective probe for visual detection of Cu<sup>2+</sup> based on 1, 8-naphthalimidederivative. *Sens. Actuat. B—Chem.* **2018**, *265*, 234–241. [[CrossRef](#)]
47. Xiong, J.J.; Huang, P.C.; Zhou, X.; Wu, F.Y. A highly selective and sensitive “turn-on” fluorescent probe of Cu<sup>2+</sup> by p-dimethylaminobenzamide-based derivative and its bioimaging in living cells. *Sens. Actuat. B—Chem.* **2016**, *232*, 673–679. [[CrossRef](#)]
48. Zhao, J.L.; Tomiyasu, H.; Wu, C.; Cong, H.; Zeng, X.; Rahman, S. Synthesis, crystal structure and complexation behaviour study of an efficient Cu<sup>2+</sup> ratiometric fluorescent chemosensor based on thiacalix[4]arene. *Tetrahedron* **2015**, *71*, 8521–8527. [[CrossRef](#)]
49. Fu, Y.; Pang, X.X.; Wang, Z.Q.; Chai, Q.; Ye, F. A highly sensitive and selective fluorescent probe for determination of Cu (II) and application in live cell imaging. *Spectrochim. Acta A* **2019**, *208*, 198–205. [[CrossRef](#)]
50. Bhorge, Y.R.; Tsai, H.T.; Huang, K.F.; Pape, A.J.; Janaki, S.N.; Yen, Y.P. A new pyrene-based Schiff-base: A selective colorimetric and fluorescent chemosensor for detection of Cu(II) and Fe(III). *Spectrochim. Acta A* **2014**, *130*, 7–12. [[CrossRef](#)]
51. Xiong, J.J.; Huang, P.C.; Zhang, C.Y.; Wu, F.Y. Colorimetric detection of Cu<sup>2+</sup> in aqueous solution and on the test kit by 4-aminoantipyrene derivatives. *Sens. Actuat. B—Chem.* **2016**, *226*, 30–36. [[CrossRef](#)]
52. Wu, N.; Zhao, L.X.; Jiang, C.Y.; Li, P.; Liu, Y.L.; Fu, Y.; Ye, F. A naked-eye visible colorimetric and fluorescent chemosensor for rapid detection of fluoride anions: Implication for toxic fluorine-containing pesticides detection. *J. Mol. Liq.* **2020**, *302*, 230–239. [[CrossRef](#)]
53. Qu, F.; Wang, F.; You, J. Dual lanthanide-probe based on coordination polymer networks for ratiometric detection of glyphosate in food samples. *Food Chem.* **2020**, *323*, 5519–5530. [[CrossRef](#)] [[PubMed](#)]